

IPC2008-64360

**EFFECTS OF SPECIMEN GEOMETRY ON FATIGUE-CRACK GROWTH RATES IN
PIPELINE STEELS***

J. M. Treinen**
NIST, Materials Reliability Division
325 Broadway
Boulder CO 80305-3328, USA

Ph. P. Darcis***
NIST, Materials Reliability Division
325 Broadway
Boulder CO 80305-3328, USA

J. D. McColskey
NIST, Materials Reliability Division
325 Broadway
Boulder CO 80305-3328, USA

R. Smith and J. Merritt
DOT/PHMSA
400 7th Street, S.W.
Washington D.C. 20590, USA

ABSTRACT

The effects of specimen geometry on the fatigue crack growth rates (FCGR) in API X65 and X100 pipeline steels were explored by use of the middle tension and compact tension specimen geometries. It was found that the specimen type has little influence on the stage II linear fatigue crack growth region for these steels. Furthermore, the FCGR behavior in the longitudinal and transverse directions was found to be nearly identical for both steels. Also of interest was a comparison of the FCGR results to the BS 7910 design curves, which showed a discrepancy between the results and the standard only at low ΔK levels. A finite element analysis of the compliance relationships used to predict the crack lengths during testing of both specimen types revealed that the expression for both the middle tension specimen and the compact tension specimen were found to be valid. Although the curved geometry of the middle tension specimen caused slightly different compliance results, these differences did not appear to affect the FCGR results.

INTRODUCTION

Fatigue properties, included in the integrity management of U.S pipeline regulations and international design standards, must be taken into consideration in the safety assessment of oil and natural gas pipelines. Fluctuations in internal operating pressure and external loads can cause fatigue crack growth [1]. Appropriate fatigue-crack-growth rate (FCGR) testing must be

performed in order to accurately use these properties in the design of the pipelines.

One such design standard is the BS7910, which uses a bilinear design curve to predict the FCGR behavior in the design process [2]. From the bilinear curve, it is possible to calculate the critical life required for the flaw to reach an unacceptable size and compare it to the total life of the structure.

Middle-crack tension, M(T), or Compact tension, C(T), specimen geometries are commonly used to measure FCGR behavior. Comparing the C(T) and M(T) specimens highlights several advantages and disadvantages in using each. Research has shown that the constraint level, or stress triaxiality at the crack tip, may influence the FCGR behavior [3]. The C(T) specimen has high constraint. The M(T), also commonly called the center-cracked tension, CCT, specimen, has a lower constraint and is more representative of the in-service conditions of the pipe.

Although the C(T) specimen has higher constraint, flat specimens can more easily be extracted in both the longitudinal and transverse directions due to their smaller size. However, unlike the M(T) specimen which has symmetrical loading on the crack, the C(T) specimen has asymmetrical loading on the crack, which is not representative of the actual loading on the pipe. Because the crack is unrestrained on one edge, the asymmetry increases as the crack grows, causing the stress intensity factor to also increase. This results in K gradient (dK/da) that is much higher in the C(T) specimen than is in the M(T) specimen. In contrast, the M(T) specimen provides full perpendicular restraint on the crack, resulting in less crack

* Contribution of an agency of the U.S. government, not subject to copyright

** current address: Paterson & Cooke, Denver CO

*** current address: Tenaris, Via Xalapa, Veracruz, Mexico

opening, a smaller K gradient, and a smaller plastic zone ahead of the crack tip as the crack grows [4].

Because of this, the M(T) specimen is generally favored for measuring basic fatigue data [4]. However, due to its large size, it is not possible to extract a flat axially-oriented specimen from the pipe without flattening the pipe, which would induce artificial plastic strains. A transversely-oriented M(T) specimen is also not possible without a special curved test fixture such as was used in [5].

Additionally, researchers have found that the FCGR behavior of different metals varies depending on the specimen orientation [6, 7]. The thermo-mechanically controlled processing (TMCP) of both steels in this study introduces complex residual stresses and plastic strain histories that may affect the FCGR behavior in different material orientations.

This study explores the FCGR curves resulting from both M(T) and C(T) specimens, along with a comparison of FCGR behavior in the longitudinal and transverse directions using API grade X65 and X100 pipeline steels. A discussion of results in comparison to the BS 7910 design standard, as well as an analysis of the geometric effects on the compliance relationship, will also be highlighted.

EXPERIMENTAL SETUP

To explore the geometry effects, if any, between using M(T) type specimens and C(T) type specimens, fatigue crack growth rate (FCGR) tests were performed with a servo-hydraulic fatigue machine according to ASTM E647-00 standard test methods [8]. The tests were completed using a stepwise increasing delta K (normalized K gradient of 0.1 mm⁻¹) control with a constant loading ratio K_{min}/K_{max} of 0.4, where the K_{min} and K_{max} are calculated from the minimum and maximum loads. All specimens were tested at 10 Hz.

The crack length was measured using the compliance method of ASTM E647-00. For the M(T) specimen this expression is defined by the following 4th order polynomial:

$$\frac{2a}{W} = C_1 u_x + C_2 u_x^2 + C_3 u_x^3 + C_4 u_x^4 \quad (1)$$

where a is the half crack length, W is the specimen width, $C_1 = 1.06905$, $C_2 = 0.588106$, $C_3 = -1.01885$, and $C_4 = 0.361691$ are compliance coefficients, and u_x is calculated as:

$$u_x = 1 - e^{-\frac{\sqrt{(EBC+\eta)(EBC-\eta+c_1\eta+c_2\eta^3)}}{2.141}}, \quad (2)$$

where E is Young's Modulus, B is the specimen thickness, C is the compliance (COD/Load), and η is $2y/W$, where COD is the crack opening displacement, and y is the distance from the crack to the point where the COD is measured (half of the gauge length).

For the C(T) specimen, ASTM 647-00 uses a fifth order polynomial for the crack length-compliance relation given by:

$$\frac{a}{W} = C_0 + C_1 u_x + C_2 u_x^2 + C_3 u_x^3 + C_4 u_x^4 + C_5 u_x^5, \quad (3)$$

where the compliance coefficients are defined as $C_0 = 1.0002$, $C_1 = -4.0632$, $C_2 = 11.242$, $C_3 = -106.04$, $C_4 = 464.33$, $C_5 = -650.68$, and u_x is defined by:

$$u_x = \frac{1}{\sqrt{BEC} + 1} \quad (4)$$

where B , E and C are defined the same as for the M(T) specimen. To prevent crack closure and other nonlinearities from influencing the compliance measurement, the automated test software excludes the top 10 % and bottom 20 % of the COD vs. load curve to measure the compliance, B . Furthermore, to average possible hysteresis effects, the compliance was measured from both the loading and unloading portions of the cycle [1,9]. An analysis of the effect the compliance expressions have on the results will be analyzed later.

The stress intensity range was calculated for the M(T) specimens as [8]:

$$\Delta K = \frac{\Delta P}{B} \sqrt{\frac{\pi a}{W^2} \sec\left(\frac{\pi a}{W}\right)} \quad (5)$$

The C(T) specimen stress intensity range is calculated using [8]:

$$\Delta K = \frac{\Delta P}{B\sqrt{W}} f\left(\frac{a}{W}\right), \quad (6)$$

where

$$f\left(\frac{a}{W}\right) = \frac{2 + \left(\frac{a}{W}\right)}{\left(1 - \frac{a}{W}\right)^{3/2}} \left[0.886 + 4.64\left(\frac{a}{W}\right) - 13.32\left(\frac{a}{W}\right)^2 + 14.72\left(\frac{a}{W}\right)^3 - 5.6\left(\frac{a}{W}\right)^4 \right]. \quad (7)$$

The M(T) specimens had the dimensions shown in Figure 1. They were full pipe-wall thickness specimens and, because of this, retained their curvature. Flattening would introduce plastic strain effects that may influence the FCGR behavior. To accommodate the curved specimens, special adaptor blocks were machined so the specimens could be mounted in the hydraulic grips [1].

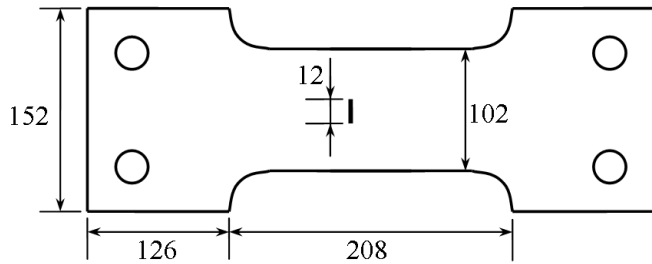


Figure 1. M(T) specimen dimensions (in mm)

The C(T) specimens dimensions are shown in Figure 2. All specimens had a thickness of 15 mm, which was within the limits of the ASTM E647 requirements.

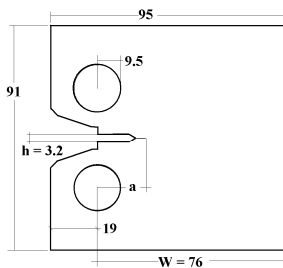


Figure 2. C(T) specimen dimensions (in mm)

Two steels, API X65 and X100, were used for the analysis. Table 1 highlights the geometry of the pipes from which the specimens were extracted. The tensile properties can be found in Table 2 where $\sigma_{0.2}$ is the 0.2 % offset yield stress, σ_{UTS} is the ultimate tensile strength, e_u is the strain at ultimate stress and e_f is failure strain.

Table 1. Pipe Dimensions

Steel	OD (mm)	Thick (mm)
X100	1321	20.6
X65-20	508	26.3
X65-22	558	31.5

Table 2. Average Tensile Properties

Steel	Orientation	E (GPa)	$\sigma_{0.2}$ (MPa)	σ_{UTS} (MPa)	$\sigma_{0.2}/\sigma_{UTS}$
X65	L	214	522	618	0.85
	T	216	576	644	0.89
X100	L	204	732	806	0.91
	T	207	798	827	0.97

Table 2 continued. Strain behavior.

Steel	Orientation	e_u (%)	e_f (%)	e_u/e_f
X65	L	10.1	27.3	0.37
	T	6.9	24.8	0.28
X100	L	4.6	20.3	0.23
	T	4.1	19.3	0.21

RESULTS

The comparison of M(T) and C(T) FCGR results was performed using the API X65 and X100 pipeline steels with pipe dimensions shown in Table 1. Because of the large size of the M(T) specimens, they must be oriented in the longitudinal pipe direction with the crack growth in the transverse (circumferential) direction. C(T) specimens were extracted from the pipe such that they had the same transverse crack growth direction as the M(T) specimens. Figure 3 compares the da/dN vs. ΔK relationship for X100, while Figure 4 shows the same comparison for X65.

Also included in the figures is the recommended da/dN vs. ΔK relationship from the British Standard 7910 used in pipeline design [2]. The standard has both a simplified law that recommends using the Paris law with $C = 5.21 \times 10^{-23}$ $\text{MPa} \cdot \text{mm}^{-0.5}$ and $m = 3$ and a bilinear relationship, valid for $R < 0.5$, that more accurately captures the sigmoidal shape of the FCGR behavior. Both are plotted in the figure, along with the upper limit of the bilinear relationship (Mean + 2 Standard Deviations), so that the measured behavior can be compared to the recommended design practices.

These two tests provided a baseline comparison to verify that the M(T) and C(T) tests produced similar FCGR results in the same pipe orientation. From Figure 3 and Figure 4 it is clear that the M(T) and C(T) specimens produce similar FCGR results, particularly at higher values of ΔK . Again, due to their large size, the M(T) specimens can only be cut from the pipe in the longitudinal pipe direction and are thus limited to measuring the FCGR in the transverse direction. However, when considering internal pressure cycles to be the source of the fatigue in the pipelines, the behavior in the transverse direction is considered more critical. C(T) specimens are small enough to also be extracted in the transverse direction, enabling the axial FCGR behavior to be measured. Figure 5 and Figure 6 show a comparison of the fatigue properties in the transverse direction from the M(T) specimen to the properties in the longitudinal direction from the C(T) specimens.

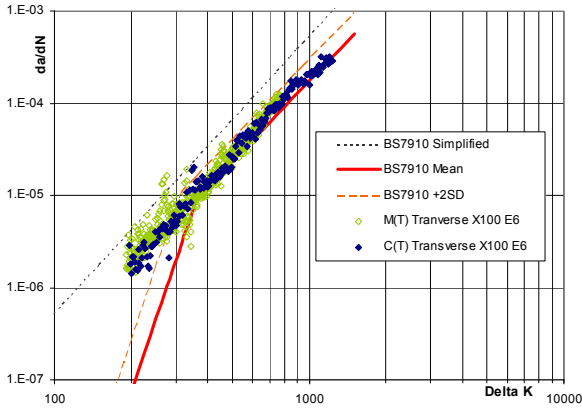


Figure 3. Comparison of C(T) and M(T) FCGR results for X100 steel to BS 7910 design standard. (Delta K in $\text{MPa}\cdot\text{mm}^{0.5}$, da/dN in mm)

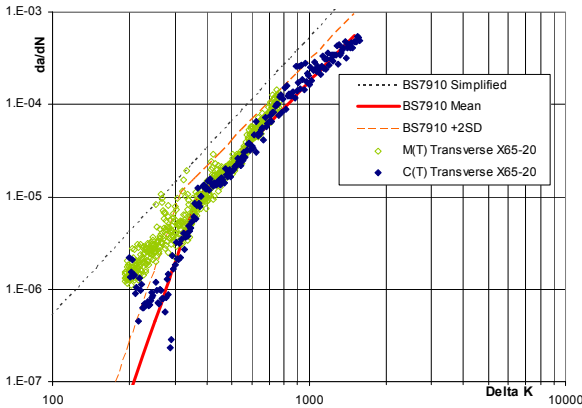


Figure 4. Comparison of C(T) and M(T) FCGR results for X65 steel to BS 7910 design standard. (Delta K in $\text{MPa}\cdot\text{mm}^{0.5}$, da/dN in mm)

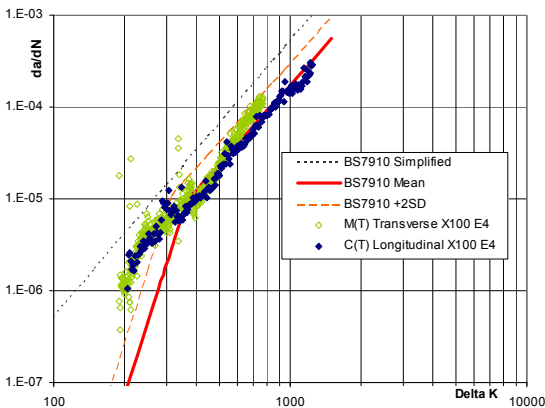


Figure 5. Comparison of FCGR results for X100 steel in Longitudinal and Transverse directions. (Delta K in $\text{MPa}\cdot\text{mm}^{0.5}$, da/dN in mm)

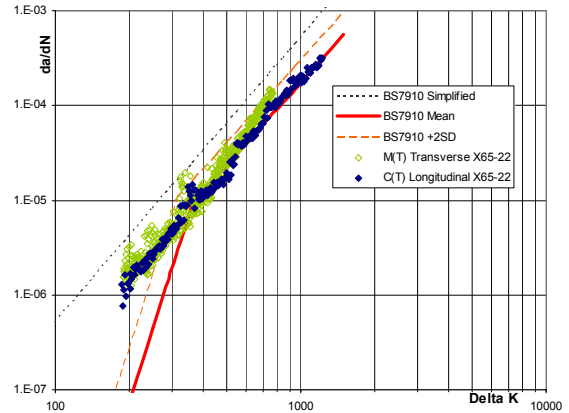


Figure 6. Comparison of FCGR results for X65 steel in Longitudinal and Transverse directions. (Delta K in $\text{MPa}\cdot\text{mm}^{0.5}$, da/dN in mm)

One general trend of the data is that results for the C(T) specimens have less scatter than the results for the M(T) specimens. This is due most likely to the simpler geometry and higher constraint of the C(T) specimen; only one crack, opposed to two in the M(T), is growing in the specimen and no curved geometric effects are present. Also of note is that the results for the M(T) specimen are slightly higher than the C(T) results.

DISCUSSION

Comparison of M(T) vs. C(T) Results

From Figure 3 and Figure 4 it appears that the specimen type has little influence on the FCGR behavior of X65 or X100 pipeline steel. It was believed that different levels of constraint may play a role on fatigue crack growth behavior, as discussed above, however this does not seem to be the case for these particular specimen geometries and materials. Additional tests need to be performed to verify this.

Comparison of Longitudinal and Transverse Results

From Figure 5 and Figure 6 it appears that little difference between the longitudinal and transverse FCGR behaviors exists. This result is expected. As Anderson explains, the stage II FCGR behavior is insensitive to microstructure or tensile properties [10], so it would be expected that for the same steel, the FCGR Stage II behavior is nearly the same, regardless of specimen orientation. However, the initiation stage of FCGR, stage I, is highly dependent on grain size and crystallographic orientations [10,11]. Because the tests performed for this study focused on the stage II crack growth, it is not possible to investigate this difference; decreasing delta K tests would need to be performed to investigate the fatigue threshold limit of the steels. These tests may reveal a difference in threshold

properties in the axial and transverse directions due to the forming processes.

Also of interest would be the effect the R-ratio has on the FCGR in the different direction. Salama has shown that considerable differences are measured in the FCGR in the different material orientations for API X60 but only at small loading ratios of 0.1. At higher ratios, the differently oriented tests produce nearly identical results [7]. Use of a loading ratio lower than 0.4, as was used in this study, may reveal differences in the FCGR behavior in the different orientations.

Comparison to BS 7910 Design standard

The results for all of the tests fall below the simplified BS 7910 design expression, verifying that the use of the simplified curve would produce conservative results. Furthermore, the C(T) data corresponds well to the second region of the standard bilinear design curve, while the M(T) data are slightly higher, but within the two standard deviation upper limit. Of particular interest is that the X65 C(T) data in Figure 4 follow the bilinear region closely, while the other results deviate from the lower linear region considerably. This deviation is likely due to the stress ratio at which the tests were performed. The bilinear region plotted is valid for $R < 0.5$. For $R > 0.5$, the knee point shifts to a smaller ΔK , while the lines also shift up. This suggests that at $R = 0.4$ the results fall between the two design curves.

Compliance/Curvature Analysis

Also of interest is the comparison of the compliance relationships for M(T) and C(T) specimens. Because the M(T) specimens were curved, the effect this curvature on the crack opening displacement (COD) in equations (1) and (2) had to be explored. This was accomplished by constructing a finite element model of the specimen geometry and incrementally adjusting the crack tip from small (8 mm) to large (36 mm) crack lengths. In addition a flat M(T) specimen was also modeled. A plot of the crack length, a , vs. the COD for both the outer diameter (OD) and inner diameter (ID) sides of the curved specimen from the finite element results, along with the prediction of a using the ASTM equation (1) above is shown in Figure 7. The figure shows the results for the X65 geometry; however, the results for the X100 geometries were similar. The loads applied to the model were the same as those applied in the actual test at each measured crack length.

From the figure, it is clear that the curvature of the specimen causes a discrepancy between the OD and ID COD values. Thus a clip gage placed on the OD will measure slightly larger COD values than a clip gage placed on the ID of the pipe. It was found that this difference between the ID and OD COD values does not significantly affect the FCGR results.

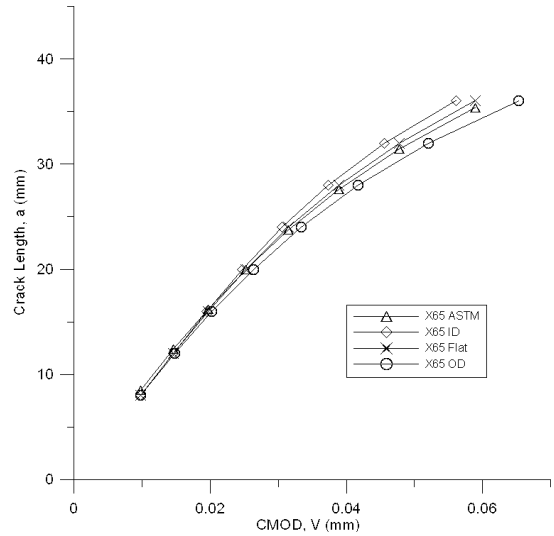


Figure 7. Comparison of FE results to ASTM prediction for the X65 M(T) specimen.

A finite element model of the C(T) specimen was also constructed to examine the validity of the ASTM compliance expression in equations (3) and (4). Since all of the C(T) specimens were flat, no curvature effects were explored. Figure 8 shows a plot of the crack length, a , vs. COD relationship found from the finite element model compared to the ASTM expression. From the figure, it is clear that the results from the finite element model are identical to those predicted by the ASTM expression; a slight over prediction of the crack length occurs initially, but the difference is small.

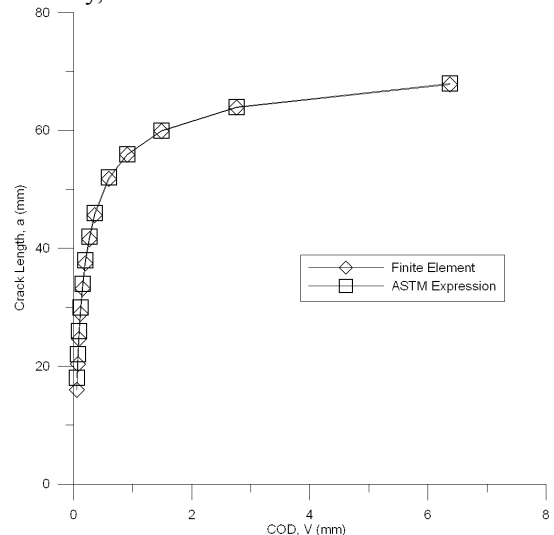


Figure 8. Comparison of the crack length vs. compliance for the ASTM expression and finite element results for the C(T) specimen.

One possible cause for the slightly higher FCGR results from the M(T) specimen in Figures 3-6 could be due to the specimen thickness. Researchers have found that the FCGR

results are dependent on the specimen thickness [4,12]. In particular, Park and Lee found that thicker specimens result in higher FCGR, which may also explain the slightly higher results in Figures 3-6, since the M(T) specimens were full-thickness (20.6 to 31.4 mm), while the C(T) specimens were only 15 mm.

CONCLUSIONS

Using both the middle tension and compact tension specimens, it was possible to explore specimen geometry effects on the FCGR of X65 and X100 pipeline steels. No difference in the behavior was found for the Stage II linear growth; however at lower loading ratios and at threshold this may not be the case. Additionally it was found that the crack growth in the longitudinal direction of the pipe is similar to that in the transverse direction. While the BS 7910 simplified design curve was conservative compared to both steels, the bilinear curve of the normal design curve predicted non-conservative da/dN rates at low ΔK values. This difference may be due to the loading ratio $R = 0.4$ being close to the limit of $R = 0.5$ for which the design curve is valid. Finally, the curvature of the M(T) specimens creates a discrepancy between the ID and OD COD results. While the difference is not significant for these particular curved geometries, use of flat C(T) specimens eliminates this effect.

ACKNOWLEDGEMENTS

The support of BP Exploration is gratefully acknowledged for providing the X100 pipeline steel, and for the permission to publish this work.

The support of US Department of Transportation, Pipeline and Hazardous Materials Safety Administration, is appreciated.

REFERENCES

- [1] Bussiba A, PhP Darcis, JD McColskey et al, 2006, "Fatigue crack Growth Rates in Six Pipeline Steels. *Proc. of the 6th IPC*, Calgary, Sept 25-29, 2006.
- [2] British Standards Institution (BSI), BS 7910-2005 "Guide to Methods for Assessing the Acceptability of Flaws in Metallic Structures" BSI, eds, London, England.
- [3] Hutar P, Seitzl S, Zdenek K, 2006, "Effect of Constraint on Fatigue Crack Propagation Near Threshold in Medium Carbon Steel" *Computational Materials Science*, 37, pp51-57.
- [4] Schijve J, 1998, "Fatigue Specimens for Sheet and Plate Material" *Fatigue and Fracture of Engineering Materials and Structures*, 21, pp347-357.
- [5] Davies P, Shewfelt R, Jarvine A, 1993, Constraint effects in testing different curved geometries of Zr-2.5Nb Pressure Tube Material" *ASTM STP 124 Constraint Effects in Fracture: Theory and Applications*, 2nd vol, eds Kirk and Bakker, pp392-424.

- [6] McMaster FJ, Tabrett CP, Smith J, 1998, "Fatigue Crack Growth Rates in Al-Li Alloy 2090. Influence of Orientation, Sheet Thickness, and Specimen Geometry" *Fatigue and Fracture of Engineering Materials and Structures*, 21, pp139-150.
- [7] Salama MM, 1994, "Effect of Orientation on Near-Threshold Crack Growth in TMCP Steels" *Proc. of the 13th OMAE Conference*, Houston, TX, Feb 27-Mar 3, vol III, pp173-179.
- [8] ASTM Standard E647-00, "Standard Test Method for Measurement of Fatigue Crack Growth Rates" 100 Barr Harbor Drive, ASTM Book of Standards, vol 03.01, West Conshohocken PA, 19428.
- [9] MTS Corporation, 2000, *Fatigue Crack Growth Manual*. Eden Prairie MN.
- [10] Anderson TL, 1991, *Fracture Mechanics*, CRC press, Boca Raton.
- [11] Vecchio RS, Crompton JS, Hertzberg RW, 1987, "The Influence of Specimen Geometry on Near Threshold Fatigue Crack Growth" *Fatigue and fracture of Engineering Materials and Structures*, 10, no 4, pp333-342.
- [12] Park HB, Lee BW, 2000, Effect of Specimen Thickness on Fatigue Crack Growth Rate" *Nuclear Engineering and Design*, 197, pp197-203.